5-18-2022

Mechanical Testing Methods for Evaluating Thermoplastic Permanent Pavement Markings

Hyungyung Jo

Matthew Giroux

Kendra Erk

Chelsea Davis

Mechanical Testing Methods for Evaluating Thermoplastic Permanent Pavement Markings

Hyungyung Jo
School of Materials Engineering
Purdue University, West Lafayette, IN, USA, 47907
Email: jo24@purdue.edu

Matthew Giroux
School of Materials Engineering
Purdue University, West Lafayette, IN, USA, 47907
Email: girouxm@purdue.edu

Kendra A. Erk
School of Materials Engineering
Purdue University, West Lafayette, IN, USA, 47907
Email: erk@purdue.edu

Chelsea S. Davis
School of Materials Engineering
Purdue University, West Lafayette, IN, USA, 47907
Email: chelsea@purdue.edu (Corresponding Author)

Word Count: 2984 words

Submitted [11/10/2021]

ABSTRACT

The durability of permanent pavement markings (PPMs) on roadways is important for drivers' safety. There are mainly two failure modes: cohesive failure that occurs internally in PPMs through small defects, such as internal pores, and adhesive failure that occurs along the interface between PPMs and road surfaces. Thus, it is critical to characterize the intrinsic mechanical properties of PPMs as well as the adhesion of PPMs on road surfaces to understand their mechanical performance and ultimately, the durability of PPMs. In this study, flexural modulus and flexural strength of PPMs was characterized via three-point bend testing, while fracture toughness was determined with single edge notch bend testing. To analyze the adhesive performance of PPMs on asphalt, a shear adhesion testing approach was developed to measure the apparent debonding energy of PPM specimens on asphalt. The shear adhesion test was performed on asphalt road surfaces and cut surfaces to investigate the chemical and mechanical interfacial effects on adhesion. Two commercial thermoplastics PPM with different mechanical properties were investigated to study how various factors directly affect the adhesion of PPMs on asphalt surfaces. Through the mechanical tests, the relationships between the intrinsic materials properties of PPMs and the mechanical performance of PPMs on asphalt were studied. A PPM material which had lower modulus and higher deformation energy exhibited greater adhesion performance on asphalt, especially when the PPM material was applied at higher asphalt surface temperatures on rough asphalt surfaces.

Keywords: Permanent pavement marking, Thermoplastic, Adhesion test

INTRODUCTION

Permanent pavement markings (PPMs) are utilized on roadways to provide clear pathways and traffic information to road users. In order to enhance driver safety, PPMs must be highly visible and durable on roadways. Understanding the mechanical properties and adhesion of PPMs is critical to predict the PPM's service lifecycle which can prevent dangerous confusion on roadways. However, there have been widespread issues in which PPMs become abraded, cracked, and peeled over time.(1)(2) Various external factors, including the condition of the roadway surface, traffic volume, and environmental conditions, can result in adhesive and cohesive failures of PPMs.(3)(4) PPM adhesion is affected by the type of pavement (material and grade) as well as the condition of the pavement (age, dryness, temperature) that it is applied to.(5)(6) PPMs can also be significantly damaged through snowplowing and salt/aggregate use in winter.(7) Internal factors also influence the performance of PPMs on different roadways, including the intrinsic material properties of the PPM (elastic modulus, tensile strength, hardness) and how these properties change in response to environmental conditions, such as variation in temperature and humidity.(8)(9)(10) However, many previous studies have focused on evaluating the retroreflectivity or the durability of PPMs based on ASTM standards using image analysis before and after a wear test. (7)(11)(12)(13) There is a lack of understanding of how the mechanical and intrinsic materials properties of PPMs affect the mechanical performance of PPMs on road surfaces.

In this study, various testing methods were utilized to quantitatively assess the mechanical performance of PPMs on asphalt using PPM thermoplastic materials. The PPM thermoplastic is known as one of the most durable pavement markings, and the second most widely used PPM in the United States.(14) The PPM thermoplastic materials behave mechanically in many different ways and often debond from road surfaces by cracking and then flaking off from the surface. Thus, the ability to resist crack propagation can be a critical factor in evaluating the durability of PPM thermoplastics. Single edge notch bend (SENB) testing was performed to determine the fracture toughness and the cohesive fracture energy of PPMs. Three-point bend (3PB) testing was also employed to measure the flexural modulus and the flexural strength of PPMs. To evaluate the adhesive performance of PPMs on asphalt, an adhesion test was developed in this study based on a Mode II in-plane shear failure. The shear adhesion test can measure the total mechanical energy, including elastic and plastic deformation in the thermoplastic PPM, required to induce the adhesive or cohesive failure of PPMs on asphalt. The performance of PPM thermoplastic is known to be sensitive to environmental conditions, such as the asphalt surface temperature at which PPM thermoplastic is applied.(5) Thus, measuring the fracture energy of PPMs on asphalt as a function of asphalt surface application temperatures could validate the new methodology as well as improve our understanding of the relationship between intrinsic properties of PPMs and the mechanical performance of PPMs on asphalt.

MATERIALS AND METHODS

Two commercially available PPM thermoplastics, labeled PPM-1 and PPM-2, were provided by Ennis-Flint, Inc. and used as-received in this study. Both PPM thermoplastic materials are comprised of approximately 80 wt% ceramic materials (calcium carbonate titanium dioxide and glass beads) in 20 wt% polymer resin. The 3-point bend (3PB) testing and the single edge notch bend (SENB) testing were utilized to characterize intrinsic mechanical properties of both PPMs. The new methodology proposed in this study to evaluate the performance of PPMs on asphalt was

the shear adhesion test on asphalt surfaces. The sample preparation procedure was based on the manufacturer recommended application instructions for each PPM. Five to six different specimens were used for each trial of all mechanical tests to obtain representative data and determine sample to sample variation.

Three-Point Bend Test and Single Edge Notch Bend Test

The 3PB test was performed to measure the flexural modulus and the flexural strength of PPMs using a universal testing machine (ADMET).

$$\sigma_{bend} = \frac{3FL}{2wd^2} \quad \text{Equation 1}$$

$$\varepsilon_{bend} = \frac{6Dd}{L^2} \quad \text{Equation 2}$$

The flexural stress, σ_{bend}, and the flexural strain, ε_{bend}, were determined by Equation 1 and 2, respectively, where F is the load, L the span, w the width, d the thickness of the specimen, and D the deflection.(15) The flexural modulus was determined by linear fitting in the elastic region, and the flexural strength was defined as the yield stress or maximum stress value.

The SENB test was conducted to determine the fracture toughness (K_{IC}), and the cohesive fracture energy (G_f). Fracture toughness indicates a materials' resistance to crack propagation. The load was applied to a notched specimen, having a 3 mm pre-crack length of the total 6 mm thick sample, in the 3PB fixture. The K_{IC} was calculated by Equation 3 when the specimen fractured,

$$K_{IC} = \frac{SF_c}{tw^{3/2}} f(\lambda) \quad \text{Equation 3}$$

where the crack shape factor is defined as

$$f(\lambda) = \frac{3\lambda^{1/2}\{1.99-\lambda(1-\lambda)(2.15-3.93\lambda+2.7\lambda^2\}}{2(1+2\lambda)(1-\lambda)^{3/2}} \quad \text{Equation 4}$$

with $\lambda = \frac{a}{W} \sim 0.5$, and F_c is the maximum load. S, t, w and a are the span length, the thickness, the width, and the pre-crack length of the sample, respectively.(16) The cohesive fracture energy, G_f, was also determined by Equation 4 based on the load-deflection graph, where U_0 is area underneath the load-displacement curve, mg is the weight of the specimen (mass multiplied by the acceleration due to gravity), d_0 is displacement at fracture, and A is the fracture surface area.(17)

$$G_f = (U_0 + mgd_0)/A \quad \text{Equation 5}$$

The mgd_0 term is assumed to be 0 since the weight of the specimen is negligible relative to the applied load. The area under the load-displacement curve represents the energy, U_0, required to fracture the specimen. For 3PB and SENB test sample preparation, a silicone mold 12 mm wide by 120 mm long and a depth of 6 mm was used. Both tests were conducted at a crosshead speed of 0.02 mm/s using a span of 80 mm.

Shear Adhesion Test

In order to evaluate the performance of PPMs on asphalt, a shear adhesion test was developed as illustrated in **Figure 1**. When applying PPM specimens on asphalt, asphalt core surface

temperatures were variously controlled at 15, 25, 35, and 40 °C using a hot-plate or a freezer. Each thermoplastic sample was heated in the mold 20 mm wide by 20 mm long and a depth of 5 mm in an oven at the manufacturer recommended application temperatures for 10 min. For PPM-2, the sample was manually agitated on a hot-plate at the application temperature prior to being transferred into the mold and heated in the oven. When removing the molded thermoplastic from the oven, the surface temperature-controlled asphalt core was placed on the melted thermoplastic and inverted, as shown in **Figure 1(a)**. A soldering iron was additionally used to locally remelt each thermoplastic specimen to fill any visible pores and remove excess thermoplastic on the asphalt core. In order to evaluate the effect of surface roughness, thermoplastic PPM specimens applied to both smooth (cut) asphalt surfaces, and rough (road) asphalt surfaces were investigated. For the shear adhesion test, asphalt cores were vertically fixed on the universal testing machine (ADMET) and the shear force was applied at a crosshead speed of 0.1 mm/s by a flat indenter to the top of the thermoplastic specimens as shown in **Figure 1(b)** until fracture was observed. The apparent fracture energy was calculated by integrating the area under the load-displacement curve. In the case that a specimen failed cohesively, the area until the maximum load at which the specimen fractured was taken as the fracture energy.

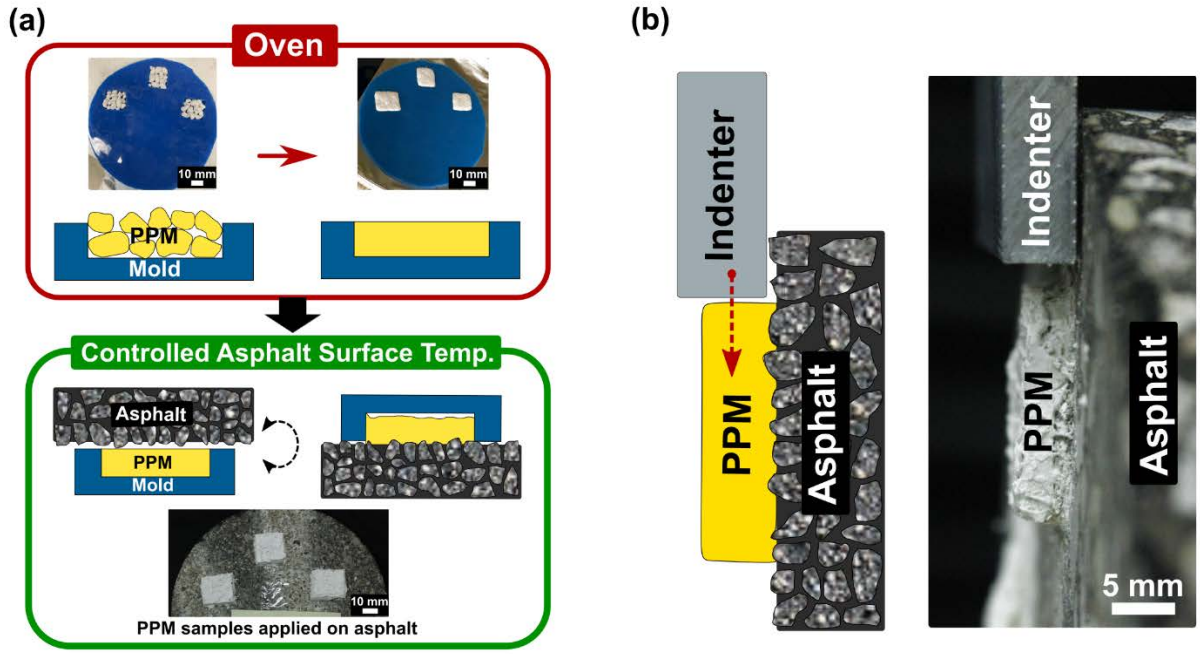

Figure 1. Schematic of permanent pavement marking (PPM) sample preparation procedure (a) and the shear adhesion test developed herein (b)

RESULTS AND DISCUSSION

Figure 2 shows representative flexural stress versus flexural strain curves for PPM-1 and PPM-2 measured from the 3PB test. Flexural moduli were determined from linear slopes of the 3PB test curves in the low strain range from 0 to 0.0005 for PPM-1, and from 0 to 0.001 for PPM-2, due to the significantly different mechanical properties and subsequent elastic deformation regimes. Flexural modulus and flexural strength values are reported in **Table 1**. Notably, the flexural modulus of PPM-1 was approximately 24 times greater than that of PPM-2, while their flexural

strength values were similar in magnitude. PPM-1 exhibited brittle fracture behavior with a high resistance to bending deformation, since the PPM-1 specimen fractured at the maximum stress with little non-linear deformation as shown in the inset graph in **Figure 2(b)**. Alternatively, PPM-2 displayed a yield point followed by plastic deformation and ultimately failed at a lower stress but much higher strain value than PPM-1. It was mainly found that the mechanical properties were significantly different; PPM-1 was brittle whereas PPM-2 was compliant having a high capacity of stress absorption and energy dissipation before fracture.

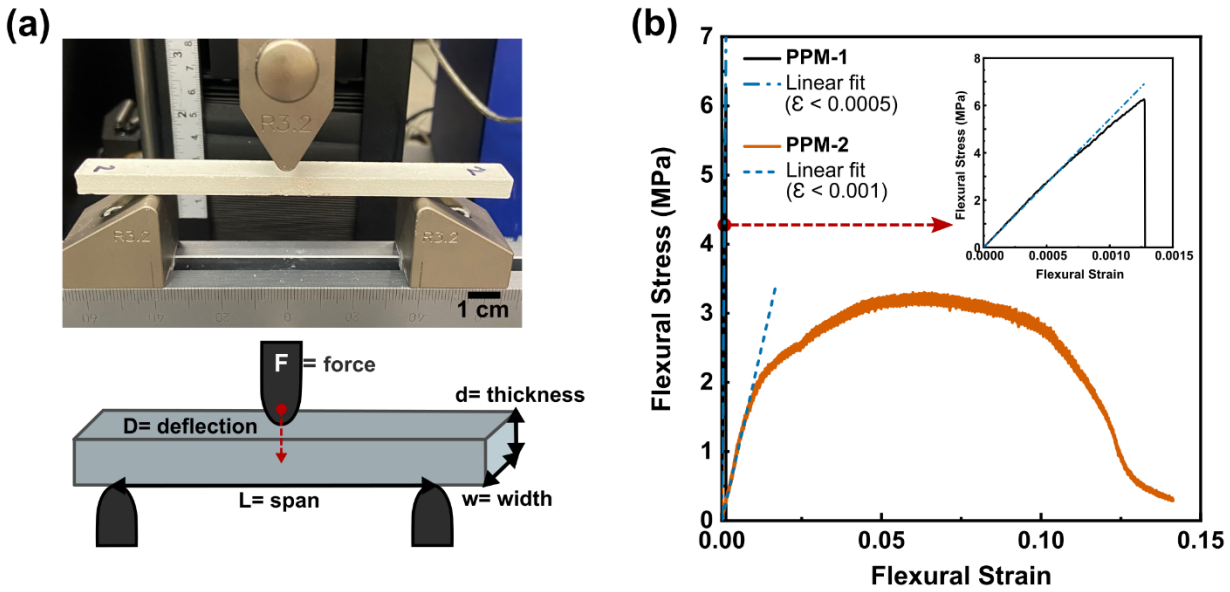

Figure 2. Photographic and schematic images (a) illustrating the 3PB test with key geometric parameters of the 3PB testing sample labelled. Flexural stress versus flexural strain curves (b) show the comparison of 3PB test results for the two PPMs. Inset in (b) shows the result of PPM-1 in greater detail.

Table 1. Flexural modulus and flexural strength of PPMs from 3PB test.

	Flexural Modulus (GPa)	Flexural Strength (MPa)
PPM-1	5.67 ± 0.69	6.66 ± 0.84
PPM-2	0.24 ± 0.05	4.00 ± 0.82

The load versus displacement curve obtained from a SENB test is shown in **Figure 3**. The fracture toughness and the cohesive fracture energy values are indicated in **Table 2**. The fracture toughness value is a function of the maximum load and the geometry of the specimen. K_{IC} values of PPM-1 and PPM-2 were within the experimental error since there was no significant difference between their maximum load values as shown in **Figure 3**. For the cohesive fracture energy, it can be calculated by dividing the integrated area under the load-displacement graph by the fracture area of the specimen, assuming that there is no plastic deformation.(17)(18) The G_f value of

PPM-1 was measured to be 0.03 ± 0.01 kN/m. However, since there was significant plastic deformation observed in PPM-2 specimens, straightforward calculation of G_f is impossible. Comparing SENB data in **Figure 3**, PPM-1 exhibited a brittle fracture behavior, since the crack propagation occurred immediately after the crack opening initiated.(19) On the other hand, the PPM-2 specimen exhibited stable crack propagation until fracture since the plastic deformation took place at the crack tip.(20) This result indicates that PPM-2 requires more energy than PPM-1 during the fracture process under the bending stress due to its higher resistance to crack propagation, as shown in **Figure 3**.

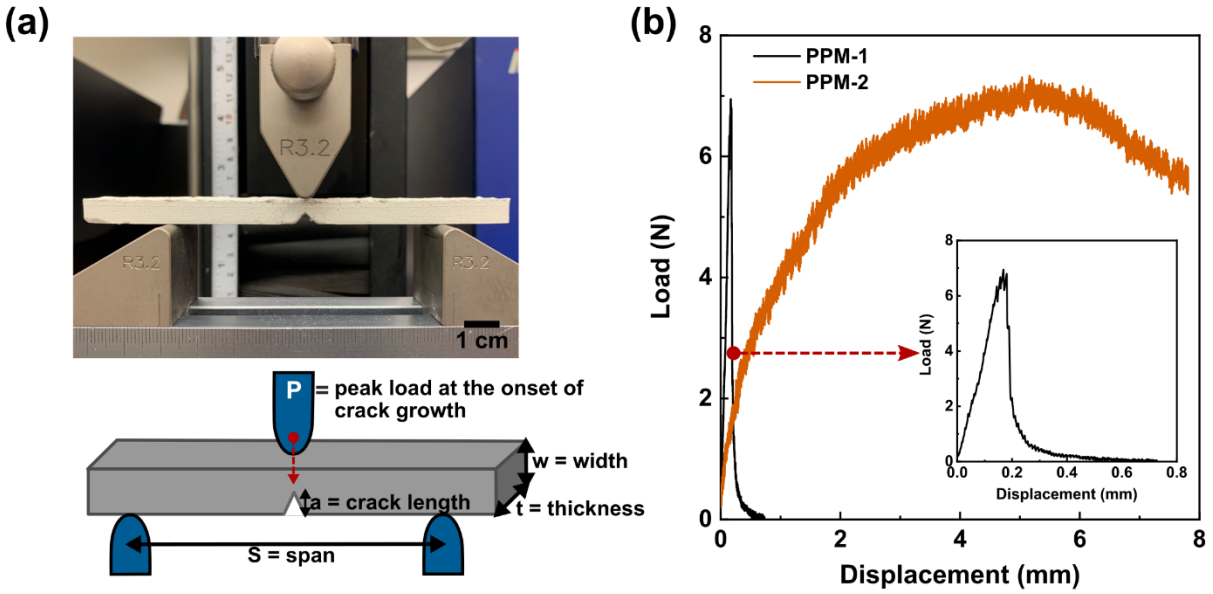

Figure 3. Photographic and schematic images (a) illustrating the SENB test with key geometric parameters of the SENB testing sample labelled. Displacement - load graph comparison for PPMs from the SENB test(b). Inset graph shows the result of PPM-1.

Table 2. Fracture toughness and cohesive fracture energy of PPMs from SENB test.

	Fracture Toughness (MPa√m)	Cohesive Fracture Energy (kN/m)
PPM-1	0.23 ± 0.04	0.03 ± 0.01
PPM-2	0.21 ± 0.03	

The shear adhesion test developed in this study determined the apparent work of debonding as the total energy required to fully remove PPM specimens from the asphalt surface. Three different failure modes resulted from the shear adhesion test: adhesive, cohesive, and mix-mode failure (shown in **Figure 4(a)**). In **Figure 4(b)**, PPM-1 specimens applied at 15 °C and 35 °C failed adhesively, while PPM-1 specimens applied at 25 °C and 40 °C failed cohesively. The slopes of graphs for PPM-1 specimens applied at 15 °C and 35°C increased until they were adhesively failed, indicating that PPM-1 exhibited the dynamic adhesive fracture behavior on asphalt. On the

other hand, all PPM-2 specimens displayed in **Figure 4(c)** were adhesively failed. The slopes of the load versus displacement data for PPM-2 significantly increased once a displacement of 2 mm was reached as the indenter came fully into contact with the top surface of the sample. As PPM-2 specimens initiated to yield, the slopes decreased until they were adhesively failed. This indicates that the PPM-2 specimen needs more energy to fracture including the elastic and plastic deformation energy, and the interfacial fracture energy.

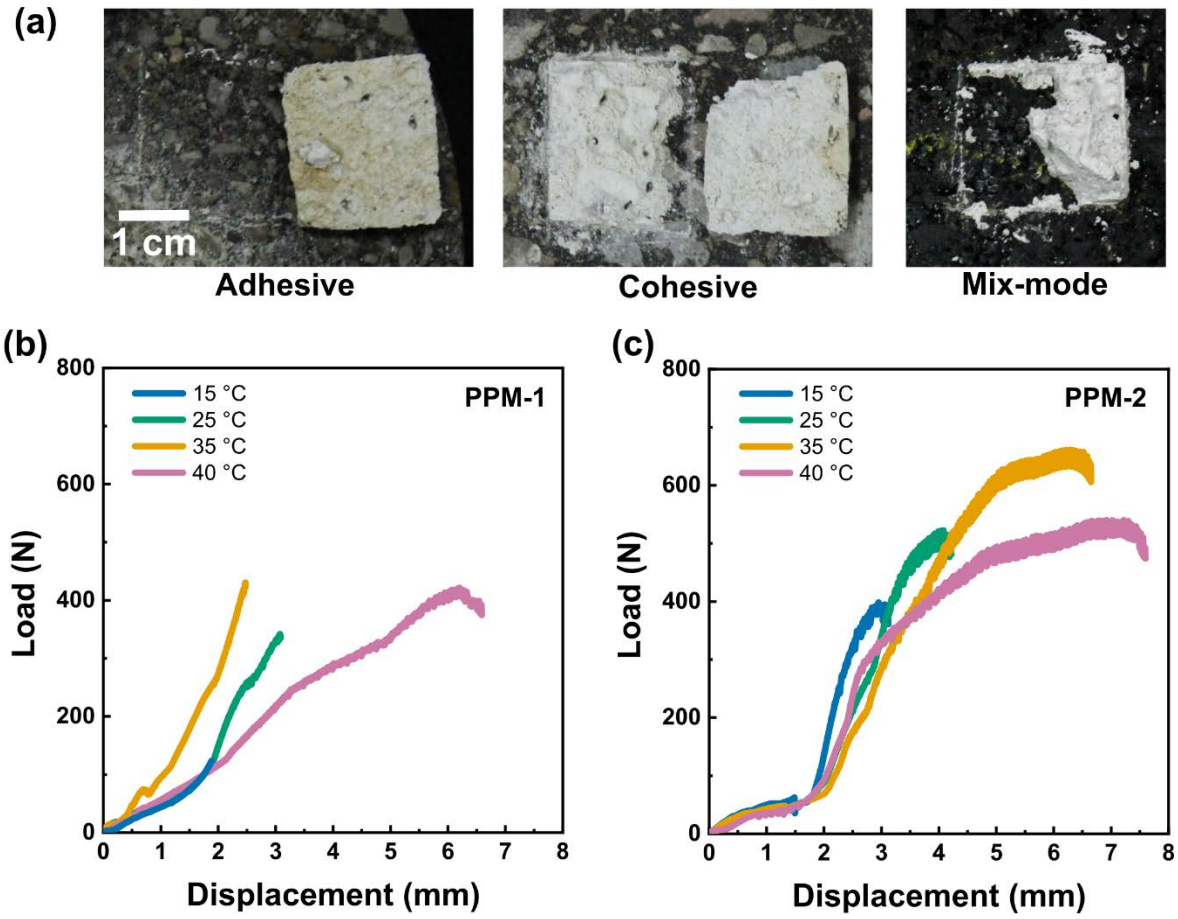

Figure 4. Photographic images (a) represent examples of fracture modes, adhesive, cohesive, and mix-mode, respectively. Shear adhesion test raw data of (b) PPM 1 and (c) PPM 2 performed on rough (road) asphalt surface at substrate application temperatures of 15, 25, 35, and 40 °C, as an example. (a) PPM-1 specimens applied at 15 °C and 35 °C failed adhesively while PPM-1 specimens applied at 25 °C and 40 °C failed cohesively. (b) All PPM-2 specimens failed adhesively.

For PPM-1 specimens tested on the smooth asphalt surface (shown in **Figure 5(a)**, most specimens applied at 15 °C and 25 °C failed adhesively, while various failure modes including the cohesive and mix-mode failure were observed for PPM-1 specimens applied at 35 °C and 40 °C. PPM-1 specimens on the rough asphalt surface (**Figure 5(b)**) also showed various failure modes and higher apparent fracture energy values than PPM-1 tested on smooth surfaces (**Figure 5(a)**).

For PPM-2, all specimens failed adhesively on the smooth asphalt surfaces, and most specimens (except two samples applied at 40 °C) also failed adhesively on the rough asphalt surface. On both smooth and rough asphalt surfaces, the fracture energies of PPM-1 and PPM-2 increased as the asphalt surface application temperature increased.

Comparing the rough and smooth asphalt surfaces, fracture energy results and thus the adhesion strength from the smooth asphalt surfaces were considered to be dominated by chemical interactions between the asphalt and PPMs. Therefore, the results indicate that as the asphalt surface application temperature increased, the degree of mechanical interlocking between the asphalt and PPMs was more likely to occur, resulting in an increase in the apparent fracture energy.(3)(6) For the shear adhesion tests on rough asphalt surfaces, since PPM specimens could more strongly mechanically interlock with the rough asphalt surfaces compared to the smooth surfaces, overall fracture energies on the rough asphalt surfaces were approximately 50% higher than analogous adhesion values on the smooth asphalt surfaces. Additionally, the results from the rough asphalt surfaces essentially reflect mechanical interactions between PPMs and asphalt. Referring back to the bending measurements presented in Figure 4, PPM-2 is compliant enough to attain more plastic deformation, resulting in the higher fracture energy, compared to PPM-1.(21) Through the shear adhesion test, it would be expected that the brittle PPM-1 will be cracked and mainly cohesively fractured whereas the more compliant PPM-2 will be plastically deformed and adhesively failed on asphalt surfaces.

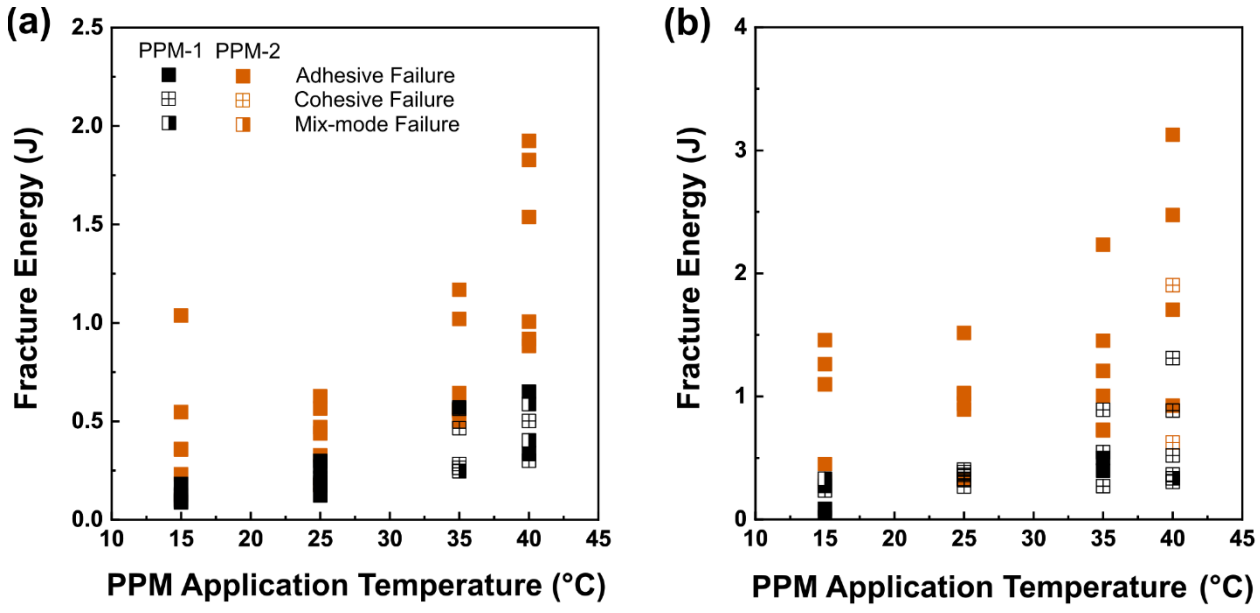

Figure 5. Comparison of shear adhesion test (a) on smooth (cut) asphalt surfaces and (b) rough (road) asphalt surfaces.

CONCLUSIONS

A shear adhesion test was developed to quantify the debonding energy of thermoplastic PPMs on asphalt surfaces. It was shown that the shear adhesion test was sensitive to differences in the adhesive performance of PPMs applied at different asphalt surface temperatures. Through the

classical mechanical characterization, PPM-1 was found to exhibit a brittle fracture behavior in which rapid crack propagation took place. Notably, the dynamic, unstable fracture in PPM-1 was observed to initiate and propagate from small defects, such as internal pores, or along the interface between glass beads and the polymer matrix. Similarly, from the shear adhesion test, PPM-1 exhibited an unstable fracture behavior on asphalt. In contrast, PPM-2, which has a relatively low flexural modulus compared to PPM-1, primarily displayed adhesive failure over the various asphalt surface application temperatures. Overall, when PPMs are able interlock mechanically with the rough asphalt surfaces, cohesive fracture mechanisms dominated the shear adhesion failure, resulting in higher fracture energies. Additionally, it was found that the environmental temperature was a critical factor affecting the adhesion between the asphalt and PPMs since the apparent fracture energy increased as the asphalt surface application temperature increased.

ACKNOWLEDGMENTS

This work was supported by the Joint Transportation Research Program administered by the Indiana Department of Transportation and Purdue University under Project Number SPR-4423. The contents of this paper reflect the views of the authors, who are responsible for the facts and the accuracy of the data presented herein and do not necessarily reflect the official views or policies of the sponsoring organizations. These contents do not constitute a standard, specification, or regulation.

AUTHOR CONTRIBUTIONS

The authors confirm contribution to the paper as follows: study conception and design: H. Jo, K. Erk, C. Davis; data collection: M. Giroux; analysis and interpretation of results: H. Jo, M. Giroux, C. Davis, K. Erk; draft manuscript preparation: H. Jo, C. Davis; All authors reviewed the results and approved the final version of the manuscript. The authors do not have any conflicts of interest to declare.

REFERENCES

1. Dwyer, C., and R. Becker. *Evaluation of Hardened Paint Pavement Markings*. Publication FHWA-AZ-020747. FHWA, Arizona Department of Transportation, 2020.

2. Xu, L., Z. Chen, X. Li, and F. Xiao. Performance, Environmental Impact and Cost Analysis of Marking Materials in Pavement Engineering, the-State-of-Art. *Journal of Cleaner Production*, 2021. 294: 126302.

3. Texas Department of Transportation. *Pavement Marking Handbook*. 2004.

4. Songchitruksa, P., G. L. Ullman, and A. M. Pike. Guidance for Cost-Effective Selection of Pavement Marking Materials for Work Zones. *Journal of Infrastructure Systems*, 2011. 17: 55–65.

5. New York State Department of Transportation. *Pavement Marking Material Guidelines New York State*. 2002.

6. Gates, T. J., H. G. Hawkins, and E. R. Rose. *Effective Pavement Marking Practices for*

Sealcoat and Hot-Mix Aspahlt Pavements. Publication FHWA/TX-03/4150-22003, Texas Department of Transportation, 2014.

7. Lee, J. T., T. L. Maleck, and W. C. Taylor. Pavement Marking Material Evaluation Study in Michigan. *Institute of Transportation Engineers (ITE)*, 1999. 69: 44–51.

8. Mirabedini, S. M., F. Zareanshahraki, and V. Mannari. Enhancing Thermoplastic Road-Marking Paints Performance Using Sustainable Rosin Ester. *Progress in Organic Coatings*, 2020. 139: 105454.

9. Mirabedini, S. M., S. S. Jamali, M. Haghayegh, M. Sharifi, A. S. Mirabedini, and R. Hashemi-Nasab. Application of Mixture Experimental Design to Optimize Formulation and Performance of Thermoplastic Road Markings. *Progress in Organic Coatings*, 2012. 75: 549–559.

10. Jiang, Y. *Durability and Retro-Reflectivity of Pavement Markings (Synthesis Study)*. Publication FHWA/IN/JTRP-2007/11, Indiana Department of Transportation, 2008.

11. Mohamed, M., A. Abdel-Rahim, E. Kassem, K. Chang, and A. G. McDonald. Laboratory-Based Evaluation of Pavement Marking Characteristics. *Journal of Transportation Engineering, Part B: Pavements*, 2020. 146: 04020016.

12. ASTM D713-12. *Standard Practice for Conducting Road Service Tests on Fluid Traffic Marking*. 1998.

13. Ozelim, L., and R. E. Turochy. Modeling Retroreflectivity Performance of Thermoplastic Pavement Markings in Alabama. *Journal of Transportation Engineering*, 2014. 140: 1–6.

14. Rasdorf, W., J. Hummer, G. Zhang, and W. Sitzabee. *Pavement Marking Performance Analysis*. North Carolina Department of Transportation, 2009.

15. Coldea, A., M. V. Swain, and N. Thiel. Mechanical Properties of Polymer-Infiltrated-Ceramic-Network Materials. *Dental Materials*, 2013. 29: 419–426.

16. Adachi, T., M. Osaki, W. Araki, and S. C. Kwon. Fracture Toughness of Nano- and Micro-Spherical Silica-Particle-Filled Epoxy Composites. *Acta Materialia*, 2008. 56: 2101–2109.

17. Malvar, L. J., and G. E. Warren. *Fracture Energy for Three-Point Bend Tests on Single-Edge Notched Beams*. 1988.

18. Gao, W., X. Liu, S. Chen, T. Q. Bui, and S. Yoshimura. A Cohesive Zone Based DE/FE Coupling Approach for Interfacial Debonding Analysis of Laminated Glass. *Theoretical and Applied Fracture Mechanics*, 2020. 108: 102668.

19. Ishikawa, M., H. Ogawa, and I. Narisawa. Brittle Fracture in Glassy Polymers. *Journal of Macromolecular Science, Part B*, 1981. 19: 421–443.

20. Duckworth, J., T. Arahira, and M. Todo. Fracture Characterization of Novel Bioceramic Microbeads Filled Polymer Composite. *Journal of Materials Science*, 2020. 55: 8954–8967.

21. Wang, H. Use of End-Loaded-Split (ELS) Test to Study Stable Fracture Behaviour of Composites under Mode II Loading. *Composite Structure*, 1996. 36: 71–79.